

Preliminary Attempt to Create a Smart Bridge Design and Implementation

C. H. Lin, M. P. Lin

Y. Y. Tsai, M. S. Tsai

Department of Civil Engineering, National Taiwan University

Advisor: C. K. Lee

Institution of Applied Mechanical, National Taiwan University

Abstract

Adopting the concept that structure dynamic properties change whenever structure undergoes deterioration, differential settlement, etc., the modal testing technique was used to examine the feasibility of using smart structure concept for early warning of structure failure. Due to the simplicity of typical bridge structure, a simple bridge model was constructed during the course of this research. Piezoelectric cables and accelerometers were used to measure the bridge vibration due to their ease of use and potential to be implemented in realistic bridges. Both time domain data and Fourier transformed frequency domain analysis techniques were used to examine the system response. Experimental data obtained clearly identified that natural frequency and mode shape changed significantly whenever the supporting bases of the bridge change.

1. Introduction

In Taiwan, the natural environment provides us with many rapid flowing rivers. The many bridges thus play an important role in the safety of our daily live, civilian or military. To identify an efficient and low cost approach to inspect the soundness of a bridge is becoming ever more important with the aging of many of our bridges. The current approaches available today, which include dispatching a driver to examine whether the bridge foundation is vacated or not, are typically troublesome and cost-prohibitive if many bridges must be inspected annually. To make thing worse, the environment that influences the soundness of the bridge is not well preserved

today in Taiwan. The high particle concentration rate within the water flows under the bridge are typically high and thus made the bridge foundation ever more difficult to observe. A simple bridge inspection will usually take more than a day not to mention many bridges are located in remote site and may take days to get access. Adopting the smart structure concept developed over the last twenty years into the bridge inspection scenario so as to identify a better approach and alleviate the above mentioned problem is one of the main focus of this article.

With the introduction of smart structure concept, the approaches developed might even be able to be extended to many other civil

engineering structures. For example, some recent outcry of the many semiconductor manufacturers related to the potential vibrations that might be generated when the planned high-speed rapid train route are found to close the new Science and Technology park in Tainan is primary related to the potential vibrations. An in-situ approach that might provide an early warning system for incoming vibrations which exceeds acceptable production standard might be useful in this situation.

The smart materials adopted in this research are piezoelectric materials. More specifically, piezoelectric sensors both in the form of accelerometers and cables are to be buried into the structure at the construction phase to create in-situ and potentially real-time monitoring of the health of the structure. In the bridge health monitoring case, it is expected that driving a testing truck through the smart bridge can create enough vibration data to determine if more detailed analysis of the bridge will be needed. If a computer or in-situ monitoring system is further connected to a piezoelectric cable buried on the bridge surface, the number of cars and even the driving speed that go through the bridge at any specific time period can also be analyzed. In this sense, the smart structure concept will be used both in the monitoring aspect and in the operational side.

As a structure changes its dynamic characteristics such as resonant frequency and mode shape, the preliminary approach adopted in this article is to use several piezoelectric sensors including piezoelectric accelerometers, acceleration rate sensors, piezoelectric cables made of VF2/VF3 (vinylidene fluoride co-polymer),^{<1>} etc., to examine the dynamic properties variations of a scale-down bridge with a

hope to shed some light in to the real structure applications. Impact hammer was used as the excitation source to perform modal testing to this scale-down model. The HP35665^{<2>} was used perform the transfer functions measurement while the STAR^{<3><4><5><6>} system to analyze data. On the strength of this, we can judge whether the bridge be destroyed or not from the analytic data to reach our intention to examine a bridge. The potential to use Finite Element Method software such as ANSYS to examine the influence of various stages of bridge destruction of a bridge is also discussed.

2. Theorem

The theoretical models used in this article will be detailed herein.

2.1. Piezoelectric Sensors and Actuators

Piezoelectric effect is a relationship between mechanical and electrical energies. Brothers Curie first discovered it in 1880.^{<7>} The piezoelectric normal effect says that stressing a piezoelectric materials will induce electric charges on the surface of the material. Adding an electric field on a piezoelectric material can to mechanical deformation is called piezoelectric reverse effect. Nowadays, more than one hundred piezoelectric materials are known, including zinc blende, calamine, boracite, sodium chlorate, PZT (lead zirconate titanate), PVDF (polyvinylidene difluoride), etc. Even bones and woods were found to possess piezoelectric property.

Piezoelectric materials can be classified into five categories, they are (1) single crystals such as quartz, (2) thin film materials such as zinc oxide, (3) polymers such as PVDF (polyvinylidene difluoride), PVF₂ (polyvinylidene Fluoride), etc., (4) ceramics such as PZT (lead zirconate titanate),

barium titanate, etc., and (5) composite materials such as PVDF-PZT.^{<8>} Different kinds of piezoelectric materials are used in different situations due to their material characteristics. For example, piezoelectric polymers are softer and more flexible and thus are better for building sensing devices.^{<9><10>} On the other hand, piezoelectric ceramics are more suitable to be used as actuators due to their high stiffness.^{<11>} The piezoelectric cable made of VF₂/VF₃ were chosen as our experimental materials due to its high sensitivity, durability and potential applicable to practical structures.

Several constants were typically used to represent the sensitivity of piezoelectric materials (Figure 1).^{<12>}

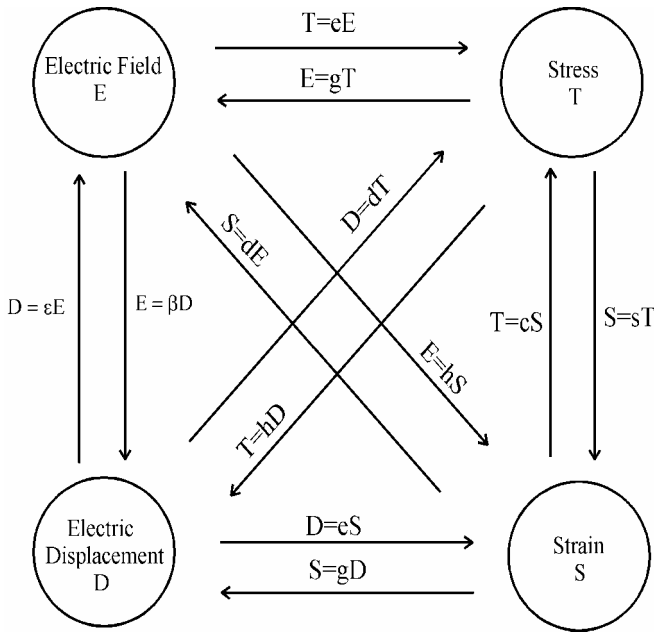


Figure 1. Piezoelectric Constants.

The constant d represents the ratio of the electric displacement and stress when the electric field is constant (D/T^E), or the ratio of the strain and the magnitude of the outer electric field when stress is constant (S/E^T). The e constant represents the ratio of the stress and the magnitude of outer electric field when strain is constant

(T/E^S), or the ratio of the electric displacement and the strain when electric field is constant (D/S^E). The g constant represents the ratio of the magnitude of inner electric field and the stress when electric displacement is constant (E/T^D), or the ratio of the magnitude of the strain and the electric displacement when stress is constant (S/D^T). The h constant represents the ratio of the magnitude of inner electric field and the strain when electric displacement is constant (E/S^D), or when strain is constant, the ratio of the stress and the electric displacement (T/D^S). In practice, if a piezoelectric material was chosen as a sensor, the g constant should be as large as possible in order to get larger signals. If a piezoelectric material was chosen as an actuator, a material with a larger d constant is usually chosen to get higher authority control.

Written the constructive equations of a piezoelectric material in IEEE compact matrix notation leads to:^{<13>}

$$S_p = s_{pq}^D T_q + g_{ip} D_k, \quad (1)$$

$$E_i = -g_{iq} T_q + \beta_{ik}^T D_k, \quad (2)$$

where $i, j, k = 1 \sim 3$ and $p, q = 1 \sim 6$ (xx, yy, zz, yz, xz, xy), the superscripts represent the fields which remain constant, T_p represents the stress and S_p represents the strain, E_i represents electric field intensity, D_i represents electric displacement, s_{pq} is the elastic compliance matrix and is the inverse of the electric stiffness matrix c_{pq} , g_{kp} represents the piezoelectric stress matrix, s_{pq} , which is the inverse of c_{pq} , represents the elastic compliance matrix, and β_{ik} is the inverse of the permittivity matrix ϵ_{ij} . These equations clearly indicate that if heat effect can be neglected, the electric field and the mechanical field of the material will be related. Typically, Eq. (1) forms the basic

piezoelectric actuator equation, and Eq. (2) forms the basic sensor equation.

Piezoelectric cables^{<14>} used in our experiment has the following cross-section (Figure 2).



Figure 2. Cross-section of the piezoelectric cable.

The piezoelectric material in the cable was made of VF₂/VF₃, which property is similar with PVDF, and belongs to the orthorhombic system. The g -constant is:

$$q_{ip} = \begin{bmatrix} 0 & 0 & 0 \\ 0 & 0 & 0 \\ 250 \times 10^{-3} & 250 \times 10^{-3} & -350 \times 10^{-3} \\ 0 & 250 \times 10^{-3} & 0 \\ 250 \times 10^{-3} & 0 & 0 \\ 0 & 0 & 0 \end{bmatrix} (Vm/N) \quad (3)$$

Since the relative dielectric constant of the piezoelectric cable is nine times to the dielectric constant of the air, i.e.,

$$\epsilon = 9 \times (8.85 \times 10^{-12}) = 7.965 \times 10^{-11} C/Vm. \quad (4)$$

From the relationship of the piezoelectric strain/charge constants:

$$d_{ip} = \epsilon_{ik} \times g_{kp} \quad (5)$$

Its d matrix is:

$$d_{ip} = \begin{bmatrix} 0 & 0 & 0 \\ 0 & 0 & 0 \\ 1.99125 \times 10^{-11} & 1.99125 \times 10^{-11} & -2.7877 \times 10^{-11} \\ 0 & 1.99125 \times 10^{-11} & 0 \\ 1.99125 \times 10^{-11} & 0 & 0 \\ 0 & 0 & 0 \end{bmatrix} (C/N) \quad (6)$$

2.2. Modal Analysis

As it was mentioned, one of the main focus of this article is to identify an efficient and proficient way to detect the safety and soundness of a structure. In this perspective, modal analysis stands out to be a good choice. For example, if a structure is damaged locally, its stiffness will decrease which lead to nature frequency decrease and damping increase. All of this change certainly will induce mode shape change. Nature frequencies, modal damping, and mode shapes are the three main structure dynamic properties that are of concern in this article. Detecting the change of these dynamic properties so as to identify the damage location and magnitude is the underlying thinking of this research.

Taking a one-degree of freedom dynamic system made of a mass m and a spring of spring constant k as the simplest model to understand the potential of the smart structure concept.^{<15><16>}

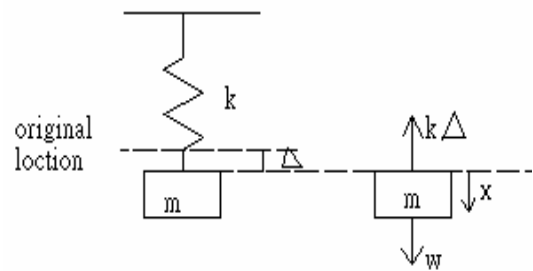


Figure 3. Illustration of a free vibration system.

Considering downward direction as positive, the

force equilibrium equation is

$$m\ddot{x} = \sum F = w - k(\Delta + x). \quad (7)$$

Equation (1) can be simplified to

$$\ddot{x} + \omega_n^2 x = 0, \quad (8)$$

where w is the weight of the object, the nature circular frequency is

$$\omega_n = \sqrt{\frac{k}{m}}. \quad (9)$$

This simple harmonic motion has general solution of the following form:

$$x = A \sin \omega_n t + B \cos \omega_n t, \quad (10)$$

where A, B is two arbitrary constants, t is time.

The period of oscillation τ_n is

$$\tau_n = \frac{2\pi}{\omega_n}. \quad (11)$$

The nature frequency f_n is

$$f_n = \frac{1}{\tau_n} = \frac{\omega_n}{2\pi} = \frac{1}{2\pi} \sqrt{\frac{k}{m}}. \quad (12)$$

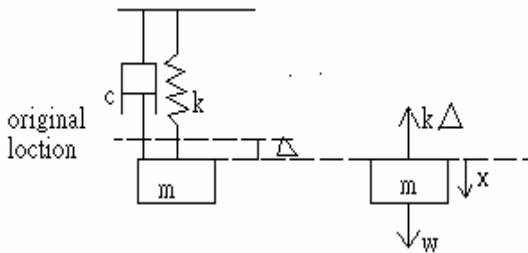


Figure 4. Illustration of a damped vibration system

Introducing damping c into the free vibration system leads to a system shown in Fig. 4. ^{<17>}

Again, adopting Newton's second Law leads to:

$$m\ddot{x} + c\dot{x} + kx = 0. \quad (13)$$

Assuming the solution takes the form of

$$x(t) = De^{\lambda t}, \quad (14)$$

where the D and λ is constant that satisfy the differential equation and its initial conditions. Substituting Eq. (14) into Eq. (13) yields:

$$\lambda_{1,2} = (-\xi \pm \sqrt{\xi^2 - 1})\omega_n, \quad (15)$$

where $\xi = c / 2m\omega_n$, and the critical damping c_{cr} equals $2m\omega_n$. When $\xi > 1$, the system is called over-damped and $x(t)$ possesses the form of an exponential decay function. In this situation, the nature frequency of the system cannot be identified. Similarly, the system is called critically damped if $\xi = 1$ and the nature frequency also cannot be identified. For the case that $\xi < 1$, the system becomes under-damped and the solution form will have oscillating period. Natural frequency can be identified in this case. More specifically, Eq. (15) can be further re-arranged to the following form

$$\lambda_{1,2} = -\xi\omega_n \pm i\omega_d, \quad (16)$$

where $\omega_d = \omega_n \sqrt{1 - \xi^2}$, $f_d = \omega_d / 2\pi$

$= \omega_n \sqrt{1 - \xi^2} / 2\pi = \sqrt{k(1 - \xi^2)} / m / 2\pi$. It is

clear from Eq. (16) that the damped frequency f_d is a function of mass, stiffness, and damping ratio

. As most civil engineering structure systems including bridges are typically under-damped, nature frequency can be used as the first step to determine the damaging conditions of a bridge.

A mode shape is associated with each natural frequency. Just like changing natural frequency may indicate structure damage, mode shapes certainly holds similar prospects. Since an aluminum bridge model supported at two ends was used in this research, a simply supported beam of length L can be used as a first order approximation to our model. The n -th mode

shape φ_n of a simply supported beam can be represented as follows:^{<18>}

$$\varphi_n = \sin \frac{n\pi}{L}. \quad (17)$$

During the scale-down bridge modal testing, an impact hammer was used to impact the model bridge, the HP35665A dynamic signal analyzer was used to record transient vibration data. By this, using the HP35665A to get the oscillation data, and the STAR system was adopted to analyze the mode shapes. Whenever a structure damage occurs, which can easily induced within the model bridge, the mode shapes will change significantly near the damaging location. It is thus expected that checking mode shape changes can identify the damaged location.

Extending the one-degree of freedom damped vibration system to a multi-degrees of freedom system, matrix notation can be used:^{<2>}

$$[M]\{\ddot{x}(t)\} + [C]\{\dot{x}(t)\} + [K]\{x(t)\} = \{0\}, \quad (18)$$

where $[M]$, $[C]$, $[K]$ are the mass, damping, and stiffness matrices. Taking Laplace transform to Eq. (18) yields

$$[B(s)]\{X(s)\} = \{0\}, \quad (19)$$

where $[B(s)] = s^2[M] + s[C] + [K]$ is called the system matrix. The equation above can be used to calculate the eigenvalues or poles by setting $[B(s)] = 0$. The poles P_k is

$$P_k = -\zeta_k + j \omega_k, \quad (20)$$

where ζ_k is modal damping of the k -th mode, and ω_k is modal frequency of the k -th mode. Its eigenvectors $[U] = [\{u_1\}, \{u_2\}, \dots, \{u_m\}]$ is the mode shapes. Introducing the external force $\{F(s)\}$ back to the previous discussions yields^{<19>}

$$\{X(s)\} = [H(s)]\{F(s)\}, \quad (21)$$

where

$$[H(s)] = \sum_{k=1}^n \frac{[r_k]}{s - p_k} + \frac{[r_k^*]}{s - p_k^*}, \quad (22)$$

p_k is the k -th pole, $[r_k]$ is the matrix of residues for the k -th pole, and the symbol “*” means complex conjugate. Using Eq. (22) as the mathematical model to perform curve fitting in order to retrieve the physical parameters of interest is the main approach adopted in STAR system.^{<6>}

2.3 Sensor Equation

The charge signal generated from the piezoelectric cable is of high impedance and thus is too small and too noisy to be detected clearly. An interfacing circuitry is usually needed to conditioning the charge signal.

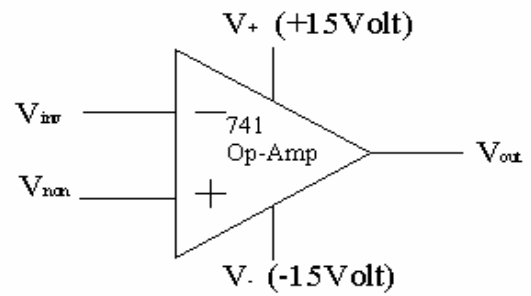


Figure 5. Illustration of a μ A741 Op-Amp

As the frequency range needed in our test is relatively low and there is no DC frequency response required, the simplest operational amplifier (Op-Amp) μ A741 (Fig. 5) was used in our experiments to serve as the basic building blocks for the amplifier.^{<20>} A two-stage amplifier was designed and fabricated. The first-stage amplifier is a simple buffer circuit, which serves to convert the piezoelectric cables output into low impedance voltage output. The second stage is a simple inverting voltage amplifier (Fig. 6).

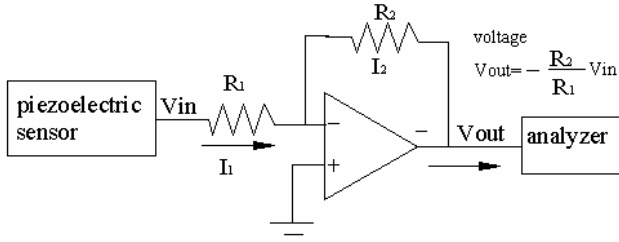


Figure 6. Illustration of a simple inverting voltage amplifier, where V_{inv} and V_{non} represent the input voltages in inverting and non-inverting channels, V_{out} represents the output voltage, V_+ and V_- connect to the power supply output.

Simple derivation based on Op-amp golden rule yields^{<21>}

$$V_{out} = 0 - I_2 R_2 = -\frac{R_2}{R_1} V_{in}, \quad (23)$$

where R_1 and R_2 are resistance of the two resistors shown, I_1 and I_2 represent the currents that flow through the resistors R_1 and R_2 , and V_{in} represent the input voltage.

Connecting the above mentioned voltage amplifier to the piezoelectric cable, the electric displacement D_i will be zero and integrating both sides of Eq. (2) yields

$$E_i ds = -g_{iq} T_q ds. \quad (24)$$

The output voltage of the piezoelectric cables could be identified to be

$$V_i = -\sum_{q=1}^6 g_{iq} \cdot Force. \quad (25)$$

Substitute Eq. (25) into Eq. (23) leads to

$$V_{out} = \frac{R_2}{R_1} \left| \sum_{q=1}^6 g_{iq} \cdot Force \right|. \quad (26)$$

It is clear from Eq. (26) that the output voltage is influenced only by the amplifier gain, the piezoelectric material g -constant, and the force. This equation will serve as the mathematical model to analyze the signal obtained from the

piezoelectric cable.

3. Experiments and Discussions

Several experiments were designed and implemented to test and verify many of the above assertions.

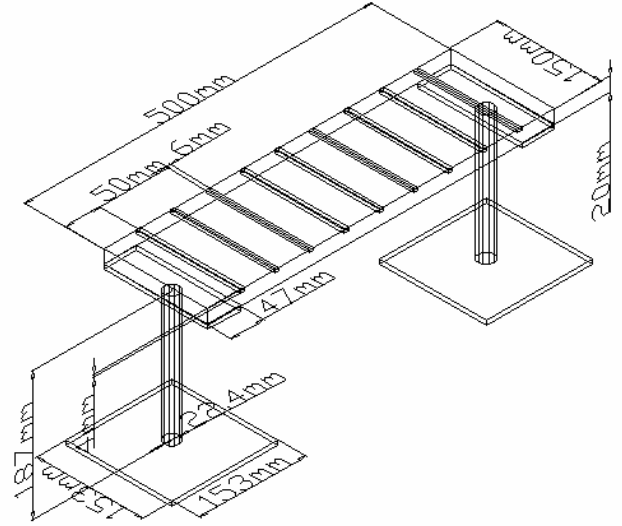


Figure 7. Schematic of the model bridge.

The experimental setups used within this research are shown in Figures 8, 9, and 10. Constructing a scale-down bridge model was the first task undertaken in order to create a testing vehicle. Materials such as gypsum, steel line, acrylic, etc. were considered to create the bridge model that can be used to simulate the concrete bridge dynamic behavior. After considering stiffness, natural frequencies, surface hardness, and referring to some references of bridge layouts,^{<22><23>} a simple aluminum based model bridge was constructed for modal testing. The mechanical layout of this model bridge makes it behave like a beam. Nine piezoelectric cables were placed into fillisters located throughout the bridge surface as it was shown in Figure 7. The +pole of the piezoelectric cable was connected to the signal side of the interfacing circuitry and the -pole of the piezoelectric cable was ground

through the interfacing circuitry. The EMI shielding layer of the piezoelectric cable was connected to the earth ground. The accelerometer was mounted on various locations of the bridge by using beeswax <24> while performing modal testing. A graphic user interface based program <25> LabVIEW was used to control the PCIMIO-data acquisition card located within the personal computer.<26> Fourier transform written in LabVIEW was used to convert the time domain signal to frequency domain. The HP35665A dynamic signal analyzer was used to obtain the gain and phase diagrams generated while performing modal testing.

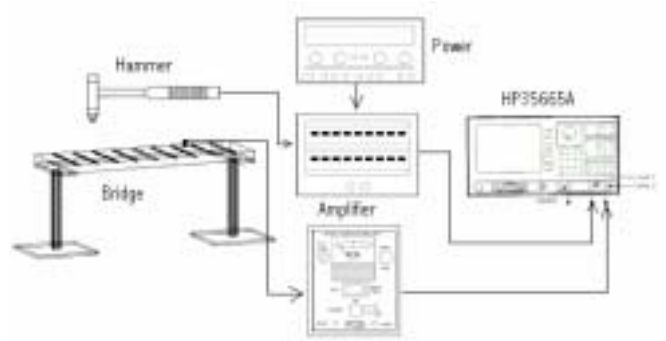


Figure 10. Experimental setup that uses the piezoelectric accelerometer as the sensor and HP35665A as the data acquisition control system.

During modal testing, the bridge model was first erected on the macadam foundation and the macadam was filled to cover the piers in order to emulate a stable and foundation sound bridge. During the second phase of the experiment, the model was erected on top of two pieces of foam rubbers to emulate an unstable or a bridge with eroded foundation. As it was described before, the impact hammer was used as the input source and either an accelerometer or a set of piezoelectric cables was used as the sensor.

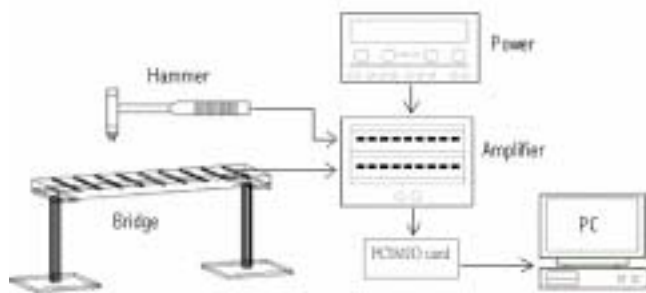


Figure 8. Experimental setup that uses the piezoelectric cables as the sensor and LabVIEW plus PC as the data acquisition control system.

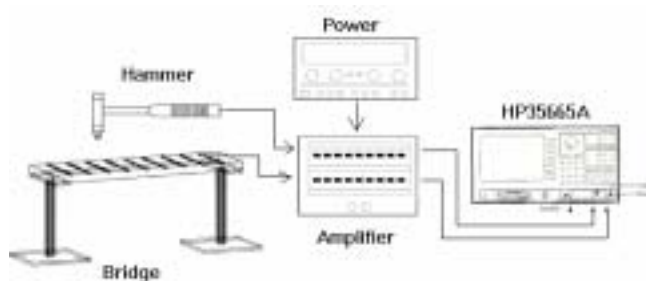
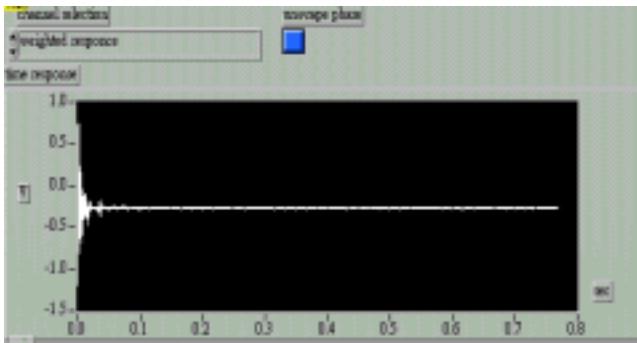
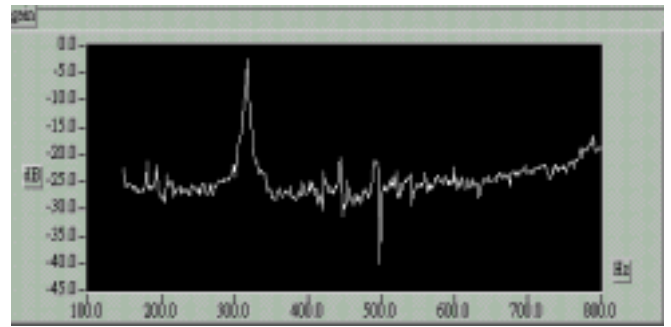


Figure 9. Experimental setup that uses the piezoelectric cables as the sensor and HP35665A as the data acquisition control system.

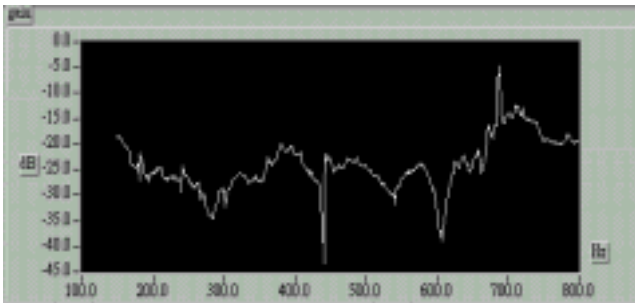
As it was described above, the experiments were done in two cases. For case 1 experiment, the base of the bridge was buried with macadam. For case 2 experiment, a soft pad was placed under the base of the bridge. It is clear from the experimental data shown in Figs. 11, 12 that impact on the two cases of experiment induce very different results. For case 1 experiment, the impulse response is short and possesses many high frequency components. For case 2 experiment, the impulse response sustains a long period of time and thus is primarily low frequency components.



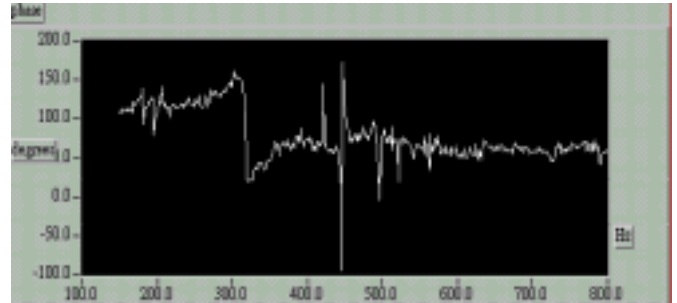
(a)



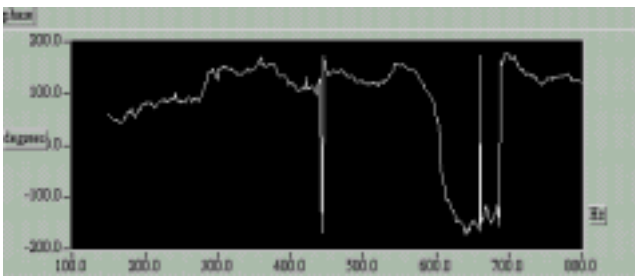
(b)



(b)



(c)



(c)

Figure 11. Time domain data (a), gain transfer function (b), and (c) phase transfer function obtained by LabVIEW when impact was introduced to case 1 experiment.

Figure 12. Time domain data (a), gain transfer function (b), and (c) phase transfer function obtained by LabVIEW when impact was introduced to case 2 experiment.

Figures 11 and 12 were obtained by using the LabVIEW program written. It is clear from these two figures that the bridge showed more damping in case 1 than in case 2. The natural frequency of case 1 is found to be around 450 Hz and the natural frequency for case 2 is about 320 Hz. This result concurs with the prediction of the simple theory mentioned above that higher damping means lower natural frequency.

Table 1. The case 1 STAR result measured by using piezoelectric cables.

Piezo cable	Freq.(Hz)	Damp.(Hz)	Damp.(%)
Stable	353.10	7.91	2.24E+00
		Mag.	Phase
Position	1	4.86E-02	82.46
	2	1.54E-02	62.50
	3	5.78E-02	65.25

	4	1.68E-03	201.29
	5	1.33E-01	239.72
	6	7.64E-02	44.47
	7	5.97E-02	52.87
	8	2.25E-03	67.24
	9	3.44E-02	44.42

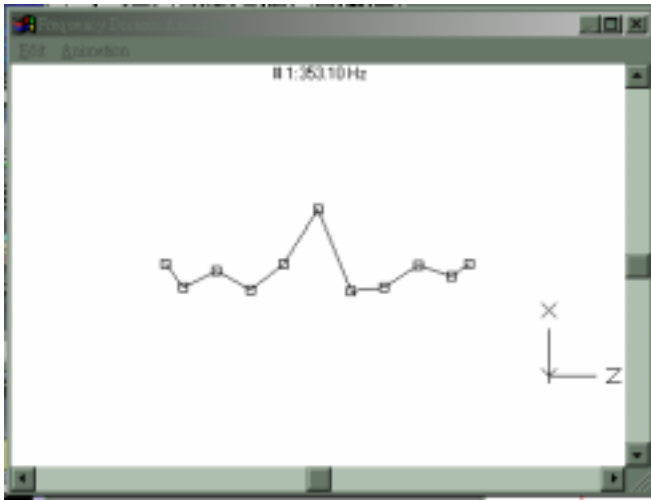


Figure 13. Mode shape of the bridge (case 1).

Table 2. The case 2 STAR result measured by using piezoelectric cables.

Piezo cable	Freq.(Hz)	Damp.(Hz)	Damp.(%)
Unstable	314.82	2.02	6.41E-01
		Mag.	Phase
Position	1	8.08E-03	266.91
	2	5.88E-03	211.66
	3	6.66E-03	325.53
	4	5.17E-03	1.37
	5	4.91E-02	18.32
	6	8.78E-03	164.71
	7	1.27E-02	174.75
	8	9.28E-04	198.21
	9	9.30E-03	16.09

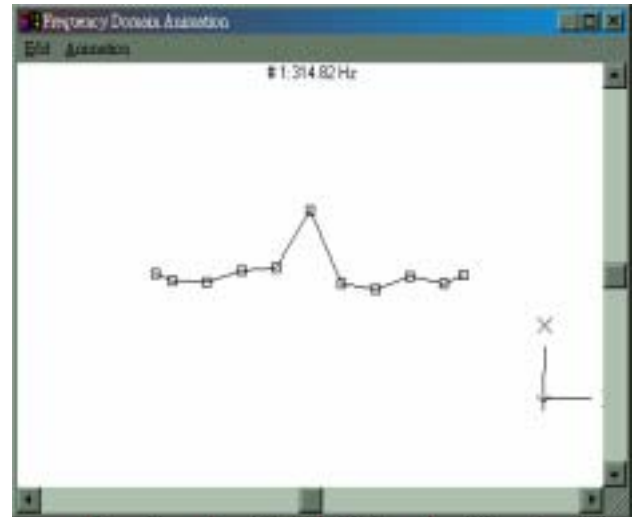


Figure 14. Mode shape of the bridge (case 2).

Table 3. STAR result for case 1.

Accelerometer	Freq.(Hz)	Damp.(Hz)	Damp.(%)
Stable	332.20	51.50	1.53E+01

Table 4. STAR result for case 2.

Accelerometer	Freq.(Hz)	Damp.(Hz)	Damp.(%)
Unstable	316.79	2.47	7.79E-01

The experimental data mentioned above indicate that when the bridge base condition was change, the overall bridge stiffness also changed. Changing from case 1 to case 2, the overall bridge system becomes softer which makes the nature frequency smaller. This result can be further examined in Tables 3 and 4, which was obtained by using accelerometer PCB 309A with serial number SN2390. Comparing the experimental results obtained from accelerometers and that of the piezoelectric cables verifies the correctness of the experiments.

4. Conclusions

Modal testing data obtained from the bridge model constructed confirms that smart structure concept may have a chance to be adopted into bridge health monitoring. It was found that as

the bridge foundation deteriorate the natural frequency of the bridge system decrease as well. With the natural frequency change, the mode shape certainly changed with it as well. Since the vibration data obtained by using piezoelectric cables and accelerometers agreed well, the correctness of the experimental data were thus verified. It is with this result that we confirm the feasibility of using mode shape and natural frequency to monitor the health of the bridge model.

5. Reference

- <1> Wang, T.T., Herber, J.M., t and Glass, A.M. "The Applications Of Ferroelectric polymers"
- <2>HP 35665A Operator's Reference, Hewlett Packard Corp., Palo Alto, California, USA, 1994.
- <3>STAR THEROY AND APPLICATIONS, Structural Measurement System, 1990.
- <4>STAR UTILITIES AND INTERFACES, Structural Measurement System, 1994.
- <5>STAR REFERENCE MANUAL, Structural Measurement System, 1990.
- <6>STAR ADVANCED CURVE FITTING REFERENCE MANUAL, Structural Measurement System, 1992.
- <7>Cady, W. G., *Piezoelectricity*, Vol. 1, McGraw-Hill, New York, pp. 1-8, 1946.
- <8>Tsai, S. W., and Hahn, H. T., *Introduction to Composite Materials*, Technomic, Penn, 1980.
- <9>Kawai, H., "The Piezoelectircity of Poly(vinylidene fluoride)," *Jpn. J. Appl. Phys.*, Vol. 8, pp. 975-976, 1969.
- <10>Murayama, N., Nakanura, N., Obara, H., and Segawa, M., "The Strong Piezoelectric in Polyvinylidene Fluoride (PVDF)," *Ultrasonics*, Vol. 14, pp. 15-23, 1976.
- <11>"Pizoflex: Compound Pizoelectirc Material," *Piezoelectric Ceramics: Piezoelectric Transducers*, Tokin America Corp., San Jose, California,1985.
- <12>林致廷, "全新點式壓電感應子之設計架構：分部式壓電感應子與點式壓電感應子之互動", 國立台灣大學應用力學研究所碩士論文, 中華民國八十七年六月。
- <13>ANSI/IEEE Standard 176, Piezoelectricity, 1987.
- <14>張育嘉, *高精密結構之線上壓電檢測系統研究*, 國立台灣大學應用力學研究所碩士論文, 中華民國八十六年六月。
- <15>William T. Thomson, *Theory of Vibration with Application*, 1985.
- <16>張世傑, *模態分析法在混凝土橋監測分析之應用*, 國立台灣大學土木工程學研究所碩士論文, 中華民國八十二年六月。
- <17>William F. Riley and Leroy D. Sturges, *engineering mechanics Dynamics*, 2nd edition,. John Wiley & Sons, Inc. 1996
- <18>Blevins. Robert D, *Formulas for Natural Frequency and Mode Shape*, Robert E Krieger Publishing CO., Inc. Krieger Drive. 1979
- <19>Mario Paz, *Structure Dynamics, Theory and Compulation*, 3rd edition Van nostrand Reinhold, New York, 1991
- <20>電子學實驗, 臺灣大學應用力學研究所, (date of publishing)。
- <21>Paul Horowitz, *Winfield Hill The Art of Electoonics*, Cambridge University, 1980
- <22> Juhani Virola, *The World's Greatest Bridge Early in the 1970's*

<23>公路橋樑設計選集, 台灣公路工程月刊社, 1962

<24>PCB Piezotronics, Inc., *Vibration & Shock Sensor Selection Guide*, 3245 Walden Avenue, Depew, New York, 14043-2495, U.S.A., 1982

<25>*Labview 5.0 for Windows 95*, National Instrument Corp. Austin, Texas.

<26>*Data Acquisition Card, Model PCIMIO*, National Instrument Corp. Austin, Texas.

們將模型橋所在的基礎改變，以模擬真實上橋樑基礎被掏空的情況，這在盜採砂石氾濫的台灣正是當務之急。此類方法除了用在橋樑上，在人造衛星或大壩上也可有不錯的應用。

6. Acknowledgement

Many people contributed to make the research work reported in this article possible. First, we would like to express our appreciation to our advisor Professor C.K. Lee for his constant support and guidance during the course of this research work. In addition, our senior classmates Miss W.H.Hsiao and Mr. H.C.Shih gave us many suggestions about this experiment. Mr. C.Y.Lee helped us about the amplifier. We owe every member of the MEMS group of Institute of Applied Mechanics, National Taiwan University for their helpful suggestions and encouragement throughout the execution of the experiment.

7. 摘要

智慧結構在最近幾年來蓬勃發展，橋樑的自動化非破壞檢測也是其中的一員，如何在短時間內以較少人力及金錢做結構檢測，是這類研究主要的目標。我們知道結構物在受到損壞時，其動態特性會有所改變，例如自然頻率、模態等。在這篇論文中，我們使用壓電線纜和加速規作為感測器，對訊號作傅利葉轉換，得到頻率域的圖形，由其中自然頻率、模態等的差異可輕易地辨別出結構物是否受到損壞，以提供較充裕的時間在發生災難前設法彌補。我